Engineering Science and Military Technologies
Volume (8) - Issue (2) - Sep 2024
ISSN: 2357- 0954
DOI:10.21608/EJMTC.2024.218487.1259

Direction finding of correlated sources in extremely low SNR environment

Original Article

Osama Ahmed Elkasrawi[1], Amr Mohamed Abdelaziz[2], Hossam El Din Abou Bakr[1], Mohamed Atta Aboelazm[1]

[1]Department of Electronic Warfare, [2]Department of Communication, Military Technical College, Cairo, Egypt

Keywords:
CRB, MUSIC, Oversampling, RMSE, USRP.

Corresponding Author:
Osama Ahmed Elkasrawi, Department of Electronic Warfare, Military Technical College, **Tel.:** 01092503269, **Email:** osama.elkasrawi@gmail.com

Abstract
Direction-Finding (DF) in low Signal-to-Noise Ratio (SNR) environments presents challenges in accurate Angle-of-Arrival (AOA) estimation, resolution, and maximum detection range due to extrinsic sources and hardware imperfections, particularly when dealing with correlated sources. Spatial-Smoothing (SS) techniques are developed to solve the problem of fully correlated sources at the expense of potential loss of both antenna aperture and angular resolution. In this paper, we introduce a pre-processing "oversampling and averaging" stage that works collaboratively with SS stage to overcome the degraded resolution performance when dealing with correlated sources. We show that oversampling intercepted signal, with an over-sampling ratio (OSR), and decimating it back to its original Nyquist rate can significantly enhance the SS-based conventional Multiple Signal Classification (MUSIC) AOA estimator's ability to resolve fully correlated sources at low SNR and narrow angular separation, which carried over a low-cost hardware environment. We derive the Cramér–Rao Bound (CRB) for AOA estimation, which shows a reduction by the same OSR factor. Simulation results at SNR= −15 dB with OSR=50, ensure a drastic drop in the Root-Mean-Square-Error (RMSE) of the MUSIC-based AOA estimator from 31◦ to 0.5◦. The resolution enhancement is confirmed by sharper peaks in the MUSIC spectrum. Simulation analysis further validates the improvement in the SS method. To demonstrate practical feasibility, we implement a prototype test-bed using the National-Instrument-Universal-Software-Radio-Peripheral (NI-USRP) Software-Defined-Radio (SDR) platform. Experimental results confirm the effectiveness of our proposed approach. Detailed mathematical analyses in the appendices support the derived results and defend our findings.

1. INTRODUCTION

DF is a critical area of research with wide-ranging applications in military and civilian domains, including radar, mobile communication, army surveillance, and security services[1–4]. Array signal processing techniques, such as Bartlett, Capon, MUSIC, Root-MUSIC, and ESPRIT, have consistently demonstrated superior performance in terms of accuracy and resolution compared to traditional methods[5–7], however, these techniques rely on acquiring an adequate number of snapshots and achieving favorable SNR, which are often challenging to attain in practical situations[2, 8].

SNR considered a critical factor in signal processing and communication systems, influencing the quality and reliability of received signals. In low SNR scenarios, the presence of noise can mask or distort the desired signal characteristics, making it challenging to extract accurate information. This issue extends to difficulties in distinguishing between different sources and determining their correlation. Consequently, accurately estimating the AOA becomes crucial but problematic due to the indistinguishability of noise and desired signal eigenvectors[9, 10].

Understanding and addressing these challenges are essential for advancing AOA estimation performance in low SNR environments. Several studies have proposed solutions to overcome the challenges of low SNR in DF. References[11,9,12] utilize DF techniques based on sparse antenna arrays to mitigate the effects of low SNR. Reference[13] profit from machine-learning, in particular the use of deep-learning, to surmount the estimation issues in low SNR conditions. Reference[14,15] improve the AOA

2357-0954 © 2024 The Military Technical College

estimation algorithms to deal with lower SNR cases. Although increasing the number of array elements and utilizing high-gain antenna elements can be advantageous, they come at an additional cost[8,16]. Similarly, increasing transmit power is beneficial, but practical constraints often limit control over the transmitter. Complicating matters further is the restricted detection range, preventing the AOA receiver from getting closer to the transmitter in many practical scenarios.

Another major challenge facing the DF methods is the presence of fully correlated signals. In real-world scenarios, even strongly correlated signals present substantial difficulties, as in multipath propagation or the use of smart jammers in military applications. As a result, DF estimators frequently underestimate the AOA, particularly in scenarios with low SNR and closely spaced targets. To address this issue, SS method has emerged as one of the most popular pre-processing techniques[1,17]. However, the SS technique suffers from effective aperture reduction, leading to decreased resolution, particularly in low SNR environments [1,5,8].

Our research suggests a potential solution to address these challenges by proposing the addition of a pre-processing stage. This stage incorporates an oversampling and averaging process, which effectively enhances the performance of AOA estimation. The approach incorporates a pre-processing stage before AOA estimation for uncorrelated sources, while for correlated sources, the pre-processing stage precedes the SS stage. Remarkably, the proposed scheme exhibits noise reduction capabilities thanks to the pre-processing gain, empirically validated as a logarithmic function of the selected OSR. Consequently, it effectively enhances the effective SNR and reduces the CRB associated with the estimator. Moreover, the proposed scheme not only enhances the resolution of the estimator but also alleviates the resolution degradation commonly observed in SS-based DF estimators. Additionally, it extends the maximum detection capability, thereby expanding the system's overall performance range. We validate the theoretical studies of the proposed AOA scheme through MATLAB-based simulations. Furthermore, experimental implementation using the NI-USRP platform corroborates the simulation results.

The subsequent sections of this paper are organized as follows, section 2 presents system modeling and problem formulation, Section 3 introduces the concept of the pre-processing stage and its gain, Section 4 provides simulation analyses supporting our findings by demonstrating enhanced AOA estimation performance using the proposed scheme, especially for nearby targets in low SNR scenarios. Additionally, the section guarantees estimation improvement when dealing with correlated sources by applying the suggested pre-processing stage prior to the SS-based MUSIC estimator. Section 5 encompasses the experimental implementation using the NI-USRP SDR platform, which confirms the effectiveness of our proposed approach. Finally, we conclude the paper in Section 6, and the appendices contain detailed mathematical analyses supporting our findings.

In the rest of the paper $(.)^H$ denotes conjugate transpose, (.)' is the first derivative, (.)" is the second derivative and (.)* is the complex conjugate. Bold uppercase letters are used to represent matrices, bold lowercase letters are used to represent vectors, and lowercase letters to represent their elements.

2. System Modelling and Problem Formulation

2.1. System Modelling

As demonstrated in fig.1, the DF receiver has intercepted a narrow-band Signal-Of-Interest (SOI) with a center-frequency F_c during a certain reception time. The SOI is incident at a certain AOA on a Uniform-Linear-Array (ULA) with *M* elements and an inter-element spacing of d. It is important to note that the results obtained with the ULA can also be applied to any other array configuration by appropriately setting the associated array response vector. ncy.

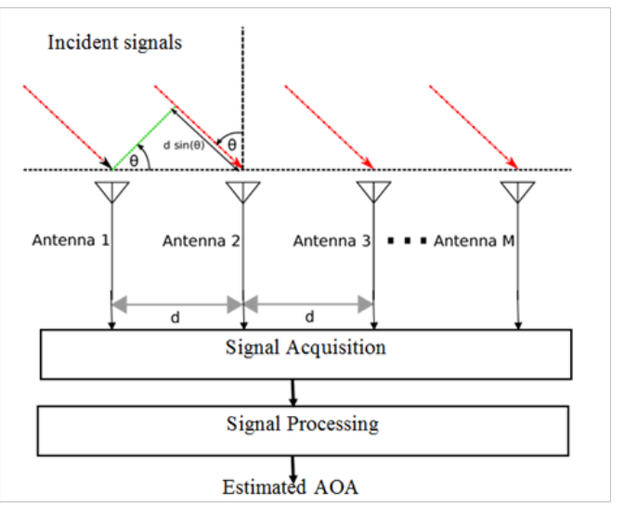

Fig. 1: System Model

The intercepted signal by M elements ULA can be represented as:

$$\mathbf{X} = \mathbf{a}(\theta)\mathbf{s} + \mathbf{N} \quad (1)$$

Where, $\mathbf{s} \in \mathcal{C}^{1\times J}$ and $\mathbf{N} \in \mathcal{C}^{M\times J}$ are J samples vector of the SOI and the noise matrix respectively. Also $\mathbf{a}(\theta) \in \mathcal{C}^{M\times 1}$ refers to the array steering vector and it can be defined as follows:

$$\mathbf{a}(\theta) = \left[1 \dots e^{-i2\pi F_c \frac{(m-1)d\sin(\theta)}{c}} \dots e^{-i2\pi F_c \frac{(M-1)d\sin(\theta)}{c}}\right]^T \quad (2)$$

Where θ is the AOA, inter-element spacing $d = \lambda_c/2$ and λ_c is the wavelength associated with the operating frequency F_c. DF algorithms based on array processing rely on correlation matrix which is defined as follows:

$$\mathbf{R} = \mathbb{E}[\mathbf{X}\mathbf{X}^H] \quad (3)$$

Given an MxM autocorrelation matrix, R, if the eigenvalues are sorted in decreasing order, the eigenvectors corresponding to the largest eigenvalues (i.e. directions of largest variability) span the signal subspace Q_s. The remaining eigenvectors span the orthogonal space, where there is only noise Q_n. These two orthogonal subspaces are then used to constitute a spatial spectrum function, MUSIC function, which detects the SOI AOA through spectral peak search. The following equation is known as MUSIC pseudo-spectrum which yields a very large value when θ equals the AOA of the corresponding SOI[1,2,6].

$$P_{MUS}(\theta) = \frac{1}{\mathbf{a}^H(\theta)\mathbf{Q_n}\mathbf{Q_n}^H\mathbf{a}(\theta)} \quad (4)$$

2.2. Problem Formulation

In scientific studies involving signal processing and communication systems, the SNR plays a crucial role in determining the quality and reliability of received signals. In low SNR scenarios, the eigenvector associated with the SOI may not be clearly distinguished from those associated with the noise. This leads to a subspace swap, where the estimated noise eigenvectors deviate drastically from the true ones[9,10]. Consequently, incorrect AOA estimation occurs, further emphasizing the impact of low SNR on the accurate discrimination of signals and noise in signal processing systems.

Considering the aforementioned reasons, this paper addresses the challenge of AOA estimation for multiple sources in environments characterized by extremely low SNR. As illustrated in fig. 2, the scenario involves a low SNR situation where a physical barrier exists between a DF receiver and two closely located targets, namely SOI_1 and SOI^2. This barrier imposes a limitation on the physical distance between the targets. The maximum effective distance between the targets and the DF receiver, in the case of LOS propagation, can be expressed as[18].

$$20\log d_1 = P_T + G_T + G_R - 32.44 - 20\log F_c - S_p \quad (5)$$

Where d_1, P_T,G_T,G_R,F_c and S_p are the maximum effective distance between targets and the DF receiver in Km, the transmitted power in dBm, transmitting antenna gain in dB,DF receiver antenna gain in dB, operating frequency in MHz and the minimum detectable signal power that can DF receiver distinguish from noise in dBm, respectively. The logarithmic form for SNR relation can be written as:

$$\alpha = S_p - \sigma^2 \quad (6)$$

By substituting with α,equation(5) can be written as

$$20\log d_1 = P_T + G_T + G_R - 32.44 - 20\log F_c - \alpha - \sigma^2 \quad (7)$$

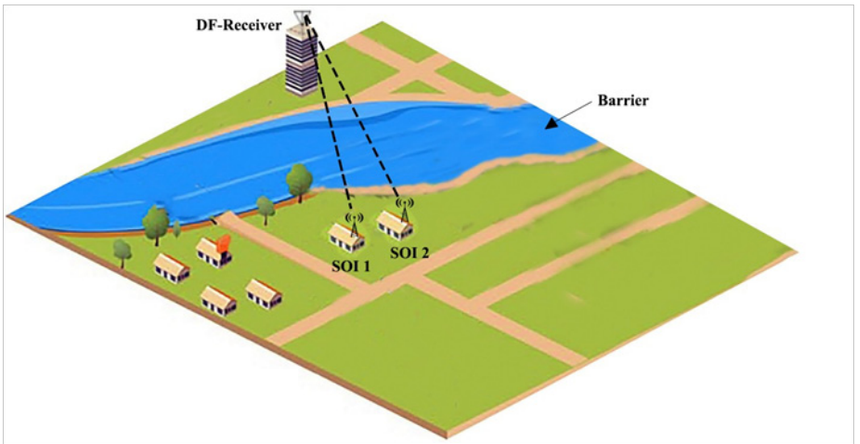

Fig. 2: Problem Formulation

Equation (7) demonstrates that by reducing the power of noise, the maximum detection range can be increased. The accuracy of estimation and the resolution are connected to CRB[19, 20], which is dependent on the noise power as illustrated in equation (8).

$$CRB \geq \frac{S_p}{2J\sigma^2(Kd\cos(\theta))^2\sum_{m=1}^{M}(m-1)^2} = \frac{1}{2J\alpha(Kd\cos(\theta))^2\sum_{m=1}^{M}(m-1)^2} \quad (8)$$

Where $K=2\pi/\lambda_c$ is the propagation constant. Therefore, decreasing the power of noise results in an increase in the effective SNR, leading to a decrease in CRB. Consequently, this improvement in CRB enhances both the estimation performance and the resolution. The derivation of equation (8) has been explained in detail in Appendix A.

The targets depicted in fig. 2 can exhibit either complete correlation or strong correlation, such as in scenarios involving multipath propagation or other real-world conditions. Consequently, the source correlation matrix may have a deficiency in rank, resulting in a reduction in the rank of the array correlation matrix[1,5]. This rank deficiency poses a challenge for accurately estimating the arrival angles of highly correlated sources using the MUSIC-based AOA estimator. Many pre-processing methods aim to address this rank deficiency in the correlation matrix or modify it to enable DOA estimation algorithms to utilize it[1,5,17,21-25]. One widely recognized pre-processing method is the SS, which is employed to decorrelate correlated sources. SS operates by partitioning the ULA into multiple smaller, overlapping subarrays and subsequently averaging the correlation matrix obtained from each subarray. By introducing random phase modulation, SS can effectively decorrelate the signals responsible for the rank deficiency[1].

$$\mathbf{R}_{ss} = \frac{1}{L_o}\sum_{b=1}^{L_o}\mathbf{R}_b \quad (9)$$

Where R_{ss} is the SS correlation matrix, R_b is the correlation matrix of the b^{th} subarray and L_o is the number of sub-arrays each of size L elements such that $L_o = M - L + 1$.
One drawback of the SS method is that it diminishes the effective aperture and degrees of freedom of the array. This reduction in effective aperture leads to an increase in the CRB, resulting in decreased estimation performance and resolution[1,5,8].

Therefore, the objective at hand is to decrease the noise power, which consequently enhances the effective SNR. This, in turn, leads to the following dependencies:

- Reduction in CRB: By reducing the CRB, there is a potential for improvement in both estimation accuracy and resolution. This helps mitigate the challenges associated with the SS method and low SNR scenarios.

- Increased maximum detection range: By increasing the maximum distance at which the DF receiver can achieve higher estimation performance and sufficient resolution, the overall system performance can be enhanced.

3. Proposed Pre-Processing Stage

The proposed scheme is based on oversampling by a sampling frequency that is integer multiple of the required Nyquist rate and then decimating it down to the initial Nyquist rate. This can be accomplished by multiplying the received over-sampled, by factor *R*, *J* signal snapshots $X \in C^{M\times JR}$, from the right, by the affine transformation matrix $V \in C^{JR\times J}$ to get:

$$\tilde{\mathbf{X}} = \mathbf{XV} \quad (10)$$

Where:

$$\mathbf{V} = \frac{1}{R}\begin{pmatrix} \mathbf{1}_{R\times1} & 0_{R\times1} & \cdots & 0_{R\times1} \\ 0_{R\times1} & \mathbf{1}_{R\times1} & \cdots & 0_{R\times1} \\ \vdots & \vdots & \ddots & \vdots \\ 0_{R\times1} & 0_{R\times1} & \cdots & \mathbf{1}_{R\times1} \end{pmatrix} \quad (11)$$

is a diagonal matrix whose diagonal elements are column vectors of dimension R.

3.1. Processing Gain

After multiplication, the down-sampled signal, $X \in C^{M\times J}$, will have a noise component whose variance is OSR less than that of $X \in C^{M\times JR}$. In particular, applying "Oversampling and Averaging" stage as a pre-processing stage results in noise variance reduction by a factor equal to the OSR, which can be expressed as[26,27].

$$\tilde{\sigma}^2 = \frac{\sigma^2}{R} \quad (12)$$

Where $\tilde{\sigma}^2$ and σ^2 are noise variance after and before applying the proposed scheme respectively and R is the OSR. Consequently, the DF receiver obtains a pre-processing gain, equals to OSR that will increase the effective SNR as indicated in the following equations:

$$\tilde{\alpha} = \frac{RS_p}{\sigma^2} = R\alpha \quad (13)$$

$$\tilde{\alpha} = \alpha + 10\log R \quad (14)$$

Where $\tilde{\alpha}$ and α are the SNR after and before applying the proposed scheme, respectively. The derivation of equation (13) and (14) have been explained in detail in Appendix C.

3.2. Cramér-Rao Bound

Noise reduction as a result of utilizing the pre-

processing stage will reduce the CRB as clarified in equation (15). This in turn will enhance both resolution and accuracy of the estimator.

$$CRB \geq \frac{1}{2J\tilde{\alpha}(Kd\cos(\theta))^2 \sum_{m=1}^{M}(m-1)^2} = \frac{1}{2J(R\alpha)(Kd\cos(\theta))^2 \sum_{m=1}^{M}(m-1)^2} \quad (15)$$

The derivation of equation (15) has been explained in detail in Appendix B.

3.3. Maximum Detection Range

The maximum distance, in Km, at which the DF receiver can correctly resolve the targets, with adequate performance and resolution, is increased by a factor that equals to the pre-processing gain, which can be calculated by substituting in equation (7) with $\tilde{\alpha}$ and can be written as following:

$$20\log d_2 = P_T + G_T + G_R - 32.44 - 20\log F_c - \alpha - \sigma^2 + 10\log R = (20\log d_1) + 10\log R \quad (16)$$

Where d_2 is the maximum effective distance between the receiver and the targets after applying the proposed scheme in Km. The derivation of equation (16) has been explained in detail in Appendix C.

4. Simulation Analysis

To validate the theoretical study, computer simulations were conducted using MATLAB. The simulation results were obtained based on the following assumptions

-Uncorrelated sources: Source signals are two narrow-band non-coherent signals, SOI1 and SOI2, with AOA equal θ_1 = -5° and θ_2 =5°, respectively. AOA estimation algorithm is the MUSIC algorithm.

- Fully correlated sources: Source signals are two narrow-band fully correlated signals, SOI1 and SOI2, with AOA equal θ_1 = -5° and -3° and θ_2 = 5° and -3° and for the case of wide and narrow angular separation respectively. AOA estimator is the SS-based MUSIC estimator.

Operating frequency *Fc* = 300 *MHz*, number of snapshots *J* = 500 snapshot, *OSR* = 50, array configuration is considered to be a ULA that composed of *M* = 6 elements, the inter-element displacement distance between ULA is d = λ/2 and finally, the signals are propagating over AWGN channel.

4.1. Pre-processing Gain Clarification

This simulation clarifies the logarithmic relation between pre-processing gain and OSR. It is clear from fig. 3 that the pre-processing gain increases slightly at high values of OSR. However, this increase comes at the cost of increased computational complexity and processing time. Moreover, as shown in fig. 3, the increment of OSR from one hundredfold to two hundredfold corresponds only to 3 dB increment of the pre-processing gain. Based on these findings, for the subsequent simulation analysis, anOSR value of 50 is selected. This choice yields a pre-processing gain of approximately 17 dB.

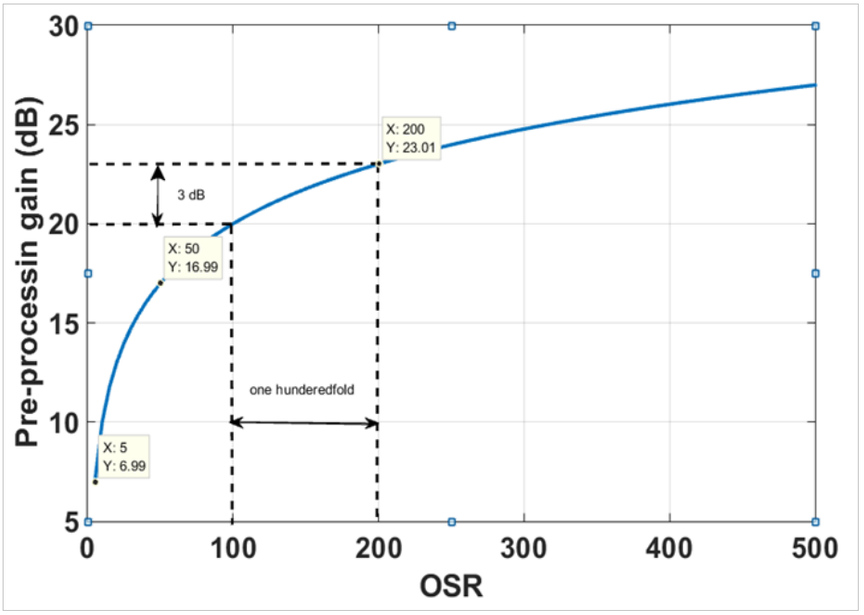

Fig. 3: Pre-processing gain as a function of OSR

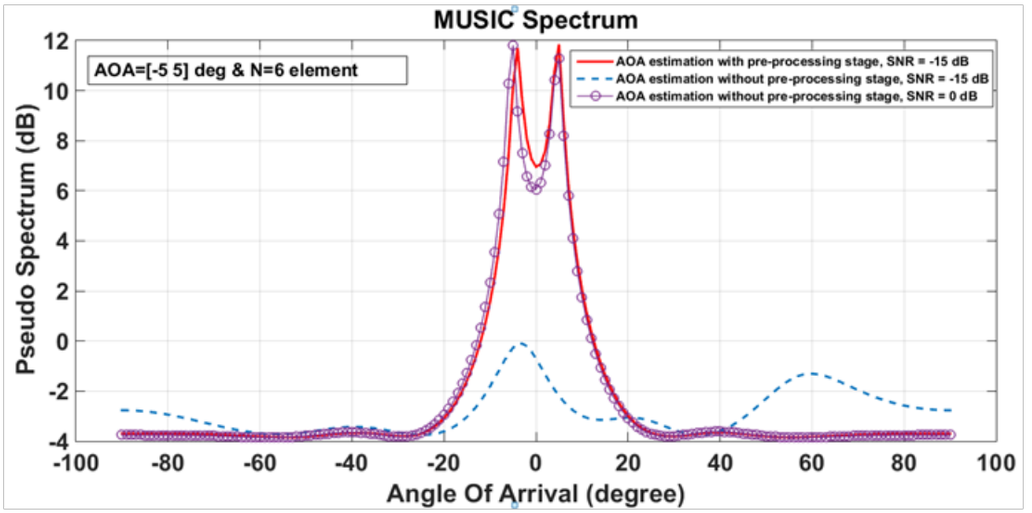

Fig. 4: MUSIC spatial spectrum before and after applying the proposed AOA estimation scheme

4.2. Uncorrelated Sources

4.2.1. Effect of the pre-processing stage on the estimation resolution

In this simulation, the estimation resolution is evaluated based on the 3 dB beam-width of the MUSIC spatial spectrum peaks. Low SNR environment was assigned to be at -15 dB. MUSIC spectrum is calculated before and after applying the pre-processing stage. It is clear from fig. 4 that MUSIC spectrum represented by the dashed line fails to resolvethe two SOIs with $\Delta\theta = 10°$ at SNR= -15 dB, while the first level of SNR at which there is a correct estimation of their angles is at SNR=0 dB as indicated by the circle-marked solid line.However, after applying the pre-processing stage with OSR = 50, MUSIC spectrum becomes able to resolve and estimate the AOAs at very low SNR= -15 dB as shown in fig. 4, which indicates the improvement in the AOA estimation resolution after applying the proposed scheme.

4.2.2. Effect of the pre-processing stage on the estimation accuracy

In this simulation, the estimation accuracy is evaluated on the basis of root mean square error (RMSE) as a function of number of array elements, number of snapshots and SNR in decibel (dB). All the results obtained in this simulation are averaged over 100 independent test runs and the SNR values are varied in the range from -15 dB to 20 dB. RMSE of the DOA estimates can be defined as[2,9,28]

$$RMSE = \sqrt{\frac{1}{100N}\sum_{k=1}^{100}\sum_{n=1}^{N}(\tilde{\theta}_n(k) - \theta_n)^2} \qquad (17)$$

Where $\tilde{\theta}_n(k)$ is the estimate of θ_n for the k-th independent test run, and N is the number of all incident signals. RMSE before and after applying the pre-processing stage, at SNR = -15 and OSR=50, is represented by the dash line curve and the solid line curve respectively as shown in fig. 5, where RMSE before applying pre-processing stage reaches 31° error but after applying it RMSE drops to 0.5° error.

These results indicate the big drop in the RMSE at low SNR values after applying the pre-processing stage, which ensures the obtained enhancement in the estimation accuracy.

To validate our results, we conducted a comparison with[14], a recent and highly cited paper addressing the same issue. Our proposed approach demonstrates a substantial advantage in terms of RMSE under low SNR conditions. In[14], a novel solution named "Enhanced Spatial Smoothing applied on Signal Subspace (ESS-SS)" was proposed, achieving an RMSE of 5 degrees at SNR= -15 dB. In contrast, our proposed approach attains a significantly lower RMSE of 0.5 degrees under similar SNR conditions, highlighting its efficacy in markedly improving the accuracy of AOA estimation in low SNR scenarios. Furthermore, a comparative examination of the CRB value reveals that our proposed approach not only achieves a lower RMSE but also closely approaches the CRB limit.

At SNR = -15 dB, the CRB bound value, as presented in[14], is 0.3 degrees, while our proposed approach achieves an RMSE of 0.5 degrees. This proximity to the CRB underscores the effectiveness of our proposed approach in approaching the fundamental limit of estimation accuracy.

These collective findings robustly affirm the strength and innovation inherent in our proposed approach, establishing it as an advanced and competitive method for AOA estimation in low SNR scenarios.

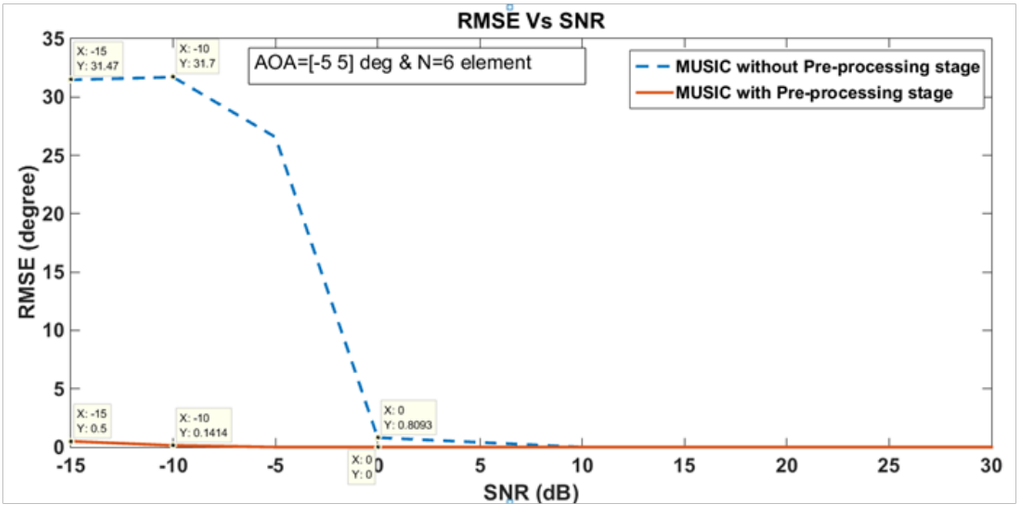

Fig. 5: RMSE as a function of SNR before and after applying the proposed AOA estimation scheme

4.3. Fully Correlated Sources

4.3.1. Effect of the pre-processing stage on the resolution of the SS-based MUSIC estimator

In this simulation, the estimation resolution is assessed using the value of the 3 dB beam width of the MUSIC spatial spectrum peaks. In fig. 6, the MUSIC spectrum is calculated for two fully correlated sources with AOA= -5° and 5° and SNR=5 dB before and after the SS method is applied. The solid line, which represents the SS-based MUSIC estimator, successfully resolves the two SOIs with $\Delta\theta = 10°$ while the dashed line, which represents the conventional MUSIC, fails to do so.

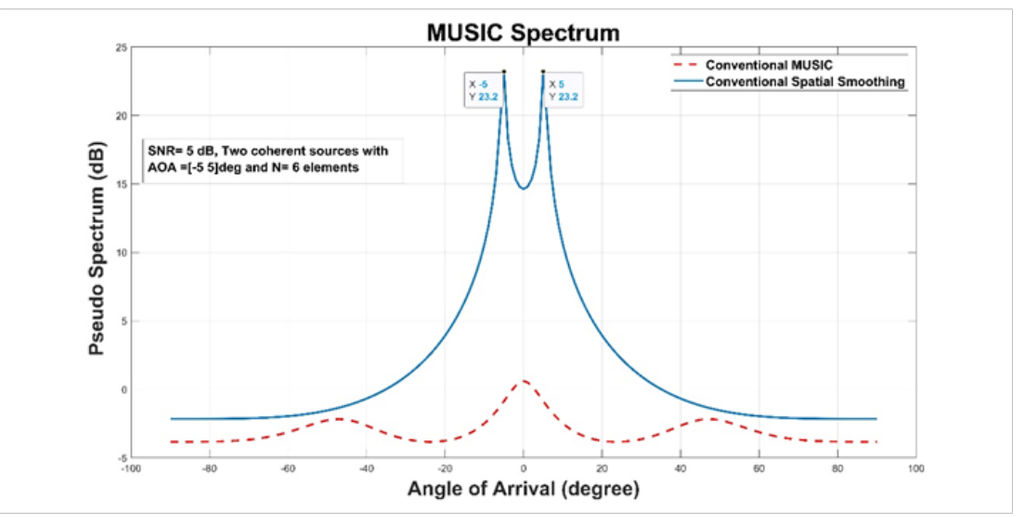

Fig. 6: The effect of SS on AOA estimation for highly correlated sources

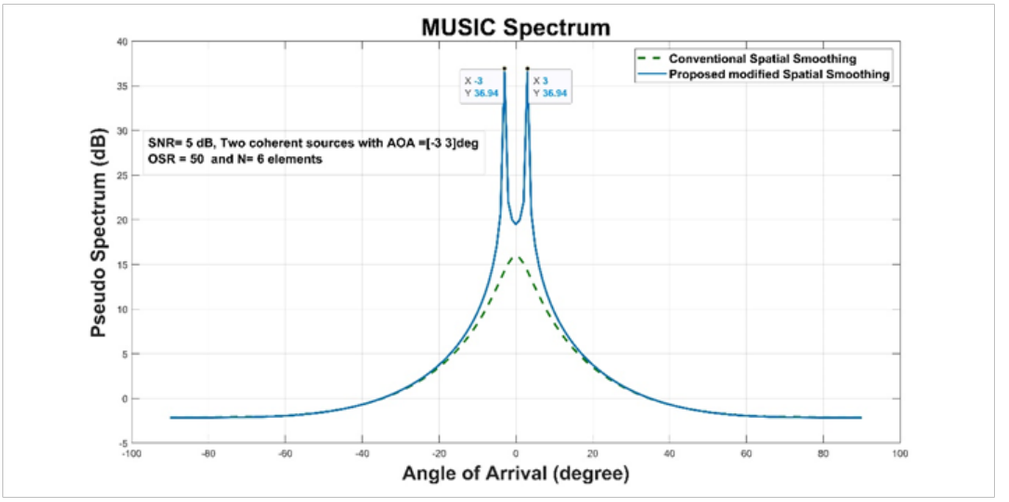

Fig. 7: Improving SS resolution

The situation of a narrow angular separation between two fully correlated sources with AOA= -3° and 3° and SNR=5 dB is illustrated in fig. 7. The two SOIs with Δθ=6° cannot be resolved using the conventional SS-based MUSIC estimator, which is depicted by the dashed line. This guarantees the resolution degradation caused by the SS method. However, after implementing the suggested pre-processing stage with OSR=50 before the SS stage, the SS-based MUSIC estimator is now able to resolve the AOAs, as shown by the solid line.

4.3.2. Enhancing the SS-based MUSIC estimator performance in low SNR scenarios

The situation of a narrow angular separation between two fully correlated sources with AOA=-3° and 3° and a low SNR scenario in which SNR=-5 dB is illustrated in fig. 8. The dashed line shows the inability of the conventional SS-based MUSIC estimator to resolve the two SOIs with Δθ = 6°. The solid line indicates that after implementing the suggested pre-processing stage with OSR=100 before the SS stage, the SS-based MUSIC estimator is now able to resolve the AOAs. This demonstrates that the SS performance degrades in low SNR scenarios and with narrow angular separation however, these difficulties can be encountered by using the suggested pre-processing stage with an appropriate OSR value.

5. Experimental Results

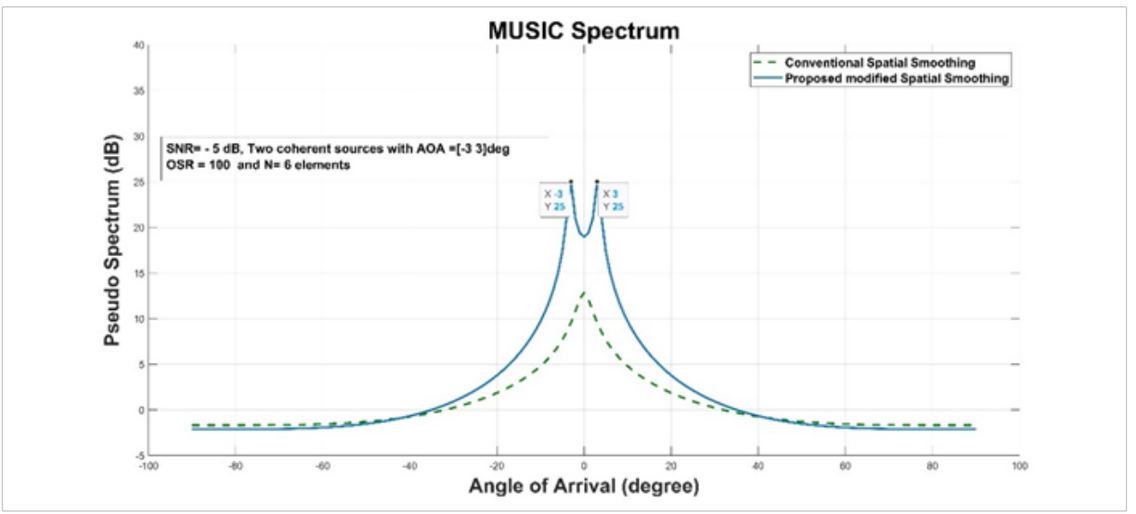

Fig. 8: SS Vs improved SS-based MUSIC estimator performance in low SNR scenarios

Table 1: List of the used parameters and their values

Parameter	Value
Center Frequency	375 MHz
Wave-length	0.8 m
Inter-element Spacing	0.5 wavelength = 0.4 m = 40cm
Array Configuration	ULA
Number of samples per fetch in receiver	100000 sample
Number of used samples for MUSIC process	1000 sample
Transmitted signal type	Tone signal
Receiver IQ rate	5MS/sec for each receiving channel
Transmitter IQ rate	400KS/sec

To demonstrate the feasibility of the proposed AOA scheme, an experimental implementation was conducted using a prototype test-bed built with the NI-USRP SDR platform and a 4-element ULA. The experimental setup block diagram is shown in fig. 9, where the target signal is generated by the USRP-X310 and the 4-element ULA, connected to theUSRP2955, functions as the DF receiver. The signal processing and control operations are performed using LABVIEW-based software on a host computer. It is important to note that the LABVIEW-based software part used in the experimental work was developed by modifying the code of published results related to the experimental setup authorized by "NATION AL INSTRUMENTS CORP.(NI)".

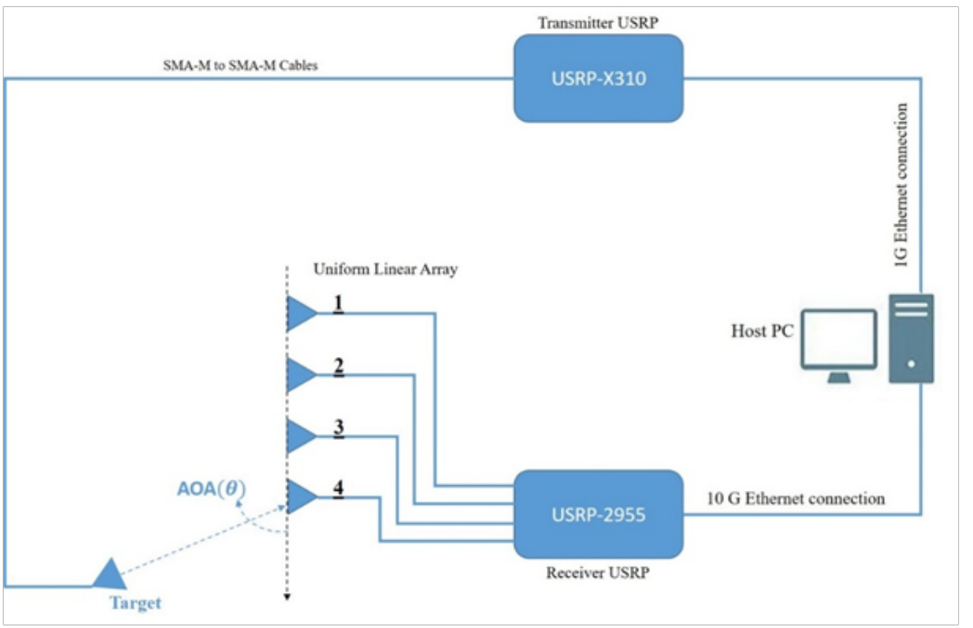

Fig. 9: Block diagram of experiment setup for verification of the proposed AOA scheme applied on 4-element ULA.

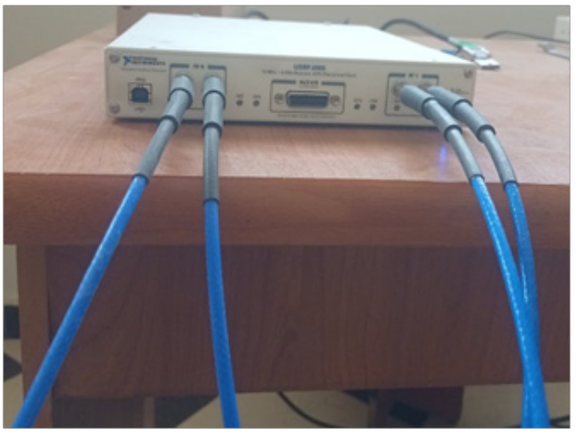

(a) USRP-2955 forming 4 channel receiver

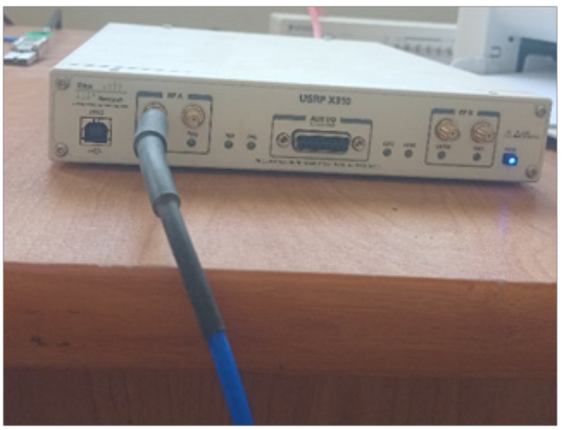

(b) USRP-X310 forming the transmitter

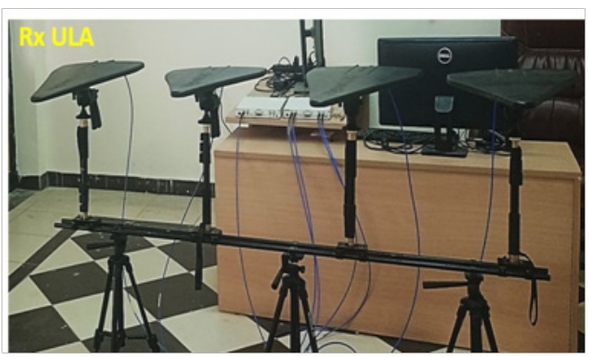

(c) Receiving antennas

(d) Transmitting antennas

Fig. 10: Test bed for experimental setup of the proposed AOA estimation scheme applied on 4- element ULA.

The original code utilized the conventional MUSIC algorithm for AOA estimation. As shown in fig. 10, testbed setup consists of using two devices of USRP platforms; 'USRP-X310' is used as a transmitter and 'USRP-2955' is the four-channel receiver. USRP-2955 has two daughter-boards of type "TwinRX daughter-boards", where each one of them has two receiving channels that construct four reception channels. These reception channels are connected to the 4-element ULA through four equal length cables of type “SMA-M to SMA-M”. These daughter-boards provide local oscillator sharing between reception paths, by which a high degree of phase synchronization can be achieved. Local oscillator sharing provides a constant repeatable relative phase offsets between reception paths, such that an initial calibration stage is needed for eradicating them. In this stage, 'a four-port RF power splitter' is used to duplicate a deterministic signal generated by a LABVIEW code. The generated signals are then direct-injected into the USRP-2955 reception paths. A LabVIEW code modification on the authorized NI-Crop. code is used to measure at once the phase differences between them as shown in fig. 11. These constants are then used by the DF receiver to make the phase calibration step. The parameters utilized in this experiment in both the transmitter and the receiver are summarized in Table 1. Experimental results shows that MUSIC spatial spectrum before applying the proposed enhancement has a wider 3dB beam width that equals approximately 31°, which indicates a degraded performance in the estimation accuracy and the resolution as shown in fig. 12. In contrast, after applying the proposed scheme, MUSIC spatial spectrum has sharper 3dB beam width that approaches 5° with approximately 16 dB pre-processing gain, which provides a significant performance advantage in the estimation accuracy and resolution as shown in fig. 13.

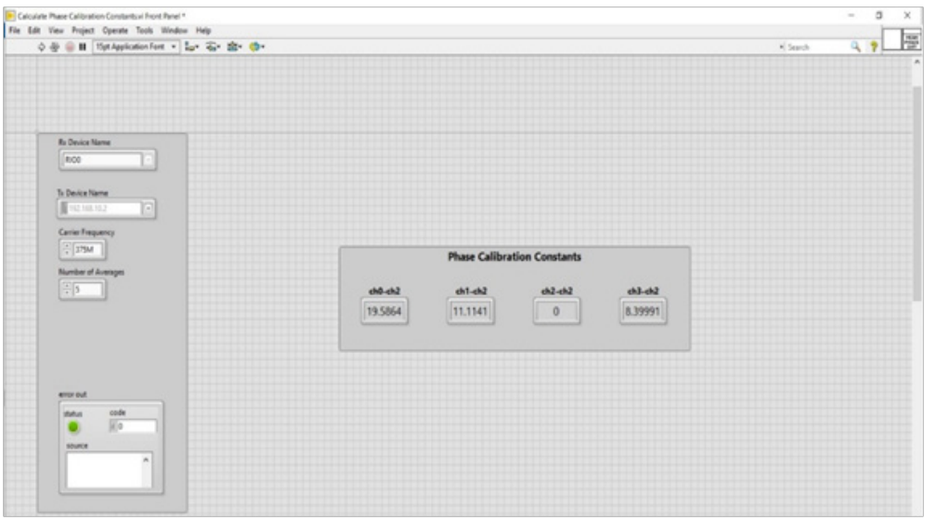

Fig. 11: Phase calibration constants Measurement

6. Conclusion

This paper introduced a novel AOA estimation scheme that improves the performance of the conventional MUSIC algorithm under low SNR conditions and enhances the estimation accuracy of the SS-based MUSIC estimator for fully correlated sources. The proposed scheme employs oversampling and averaging techniques, which result in a logarithmic increase in pre-processing gain with the chosen OSR. Simulation results confirmed the theoretical studies and validated the effectiveness of the proposed AOA estimation scheme.

The AOA estimation accuracy, measured by the RMSE value, achieved an accuracy of approximately 0.5° at an SNR of -15dB with an OSRof 50. Moreover, the proposed pre-processing gain compensates for the decrease in estimation performance resulting from the utilization of the SS method when dealing with fully correlated sources and the subsequent reduction in effective aperture. Simulation analyses provided further evidence supporting this result.

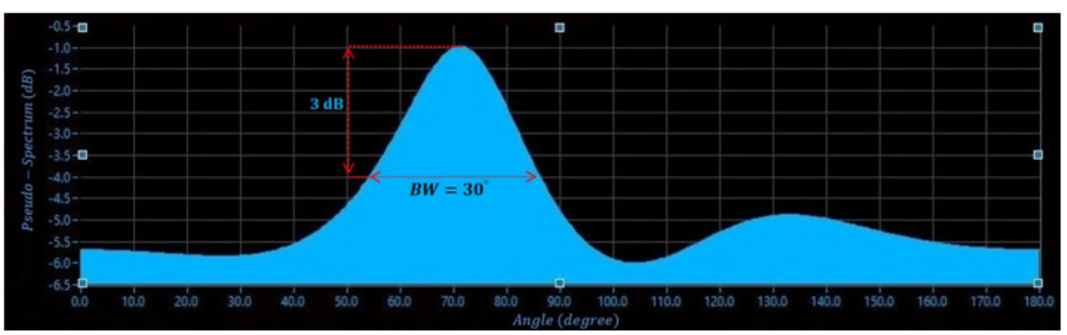

Fig. 12: Experimental result for estimating θ=68° before applying pre-processing stage

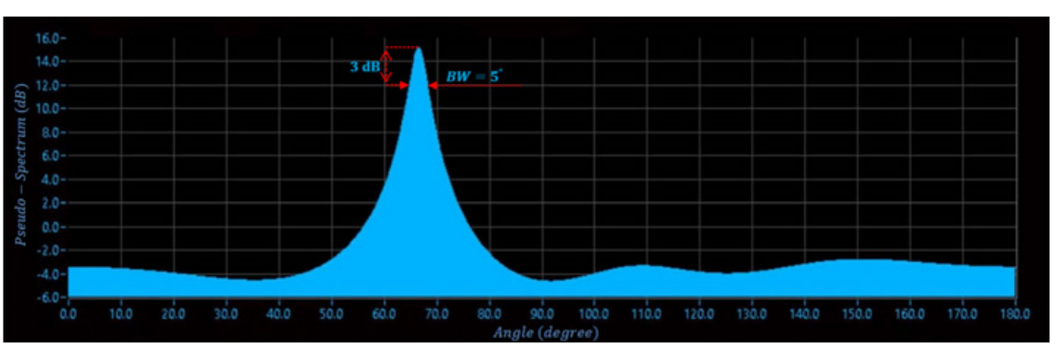

Fig. 13: Experimental result for estimating θ= 68° after applying pre-processing stage

Practical testing was conducted, taking into account the issue of phase synchronization between reception paths. The results obtained from LABVIEW simulations and experimental implementation using the USRP SDR, a commercially available low-cost and scalable platform, demonstrated the efficiency of the proposed scheme in improving the AOA estimation performance.

It is important to note that in this paper, the proposed AOA estimation scheme was verified through simulations and experimental implementation specifically for estimating single-tone Sources of Interest (SOIs). Future work will involve studying the estimation of SOI bandwidth for different signal types, where the OSR will become a dependent parameter based on the SOI bandwidth.

6. Conflicts of Interest

The work submitted in this paper is part of current Master program in Electrical Engineering at Military Technical College in Egypt .The first author is the postgraduate student and the remaining co-authors are supervisors.All authors contributed equally to this work.

7. References

[1] L. C. Godara, Smart Antennas. Boca Raton, FL: CRC Press, 2004.
A. Sharma and S. Mathur, "Performance analysis of adaptive array signal processing algorithms," IETE Tech. Rev., vol. 33, no. 5, pp. 472–491, 2016.
G. Kratschmer, "Introduction into theory of direction finding," Radiomonitoring and Radiolocation, 2010.
A. Abdelaziz, R. Burton, F. Barickman, J. Martin, J. Weston, and C. E. Koksal, "Enhanced authentication based on angle of signal arrivals," IEEE Trans. Veh. Technol., vol. 68, no. 5, pp. 4602–4614, 2019.
H. Krim and M. Viberg, "Two decades of array signal processing research: the parametric approach," IEEE Signal Process. Mag., vol. 13, no. 4, pp. 67–94, 1996.
E. Gentilho Jr, P. R. Scalassara, and T. Abrão, "Direction-of-arrival estimation methods: A performance-complexity tradeoff perspective," J. Signal Process. Syst., vol. 92, no. 2, pp. 239–256, 2020.
M. Vijay and U. L. Sunita, "An overview of smart antenna and a survey on direction of arrival estimation algorithms for smart antenna," Journal of Electronics and Communication Engineering, 2014.
H. Tang, "DOA estimation based on MUSIC algorithm," 2014.
M. Wang, "Statistical Performance Analysis of Sparse Linear Arrays," Washington University in St. Louis, 2018.
C.-L. Liu and P. P. Vaidyanathan, "Cramér–Rao bounds for coprime and other sparse arrays, which find more sources than sensors," Digit. Signal Process., vol. 61, pp. 43–61, 2017.
K. Usman, R. Magdalena, and M. Ramdhani, "Direction of arrival estimation in low SNR environment using two stages sparse reconstruction," in 2018 International Conference on Control, Electronics, Renewable Energy and Communications (ICCEREC), 2018.
K. Hameed et al., "DOA estimation in low SNR environment through coprime antenna arrays: An innovative approach by applying flower pollination algorithm," Appl. Sci. (Basel), vol. 11, no. 17, p. 7985, 2021.
G. K. Papageorgiou and M. Sellathurai, "Direction-of-arrival estimation in the low-SNR regime via a denoisingautoencoder," in 2020 IEEE 21st International Workshop on Signal Processing Advances in Wireless Communications (SPAWC), 2020.
J. Pan, M. Sun, Y. Wang, and X. Zhang, "An enhanced spatial smoothing technique with ESPRIT algorithm for direction of arrival estimation in coherent scenarios," IEEE Trans. Signal Process., vol. 68, pp. 3635–3643, 2020.
A.-S. Mohammed, "A Minimum Variance Noise Algorithm for 2D and 3D Direction Estimation in MIMO Wireless Communication Systems," in 6th International Conference on Wireless Networks and Mobile Communications (WINCOM), IEEE, 2018.
A. Abdullah and L. A. A.-R. Najim, "Comparative Study of Super-Performance DOA Algorithms based for RF Source Direction Finding and Tracking," Technology Reports of Kansai University, vol. 63, no. 2, 2021.
M. Tie-Jun and T. Wax, "On spatial smoothing for direction-of-arrival estimation of coherent signals," IEEE Transactions on Acoustics, Speech, and Signal Processing, vol. 33, pp. 806–811, 1985.
D. L. Adamy, Electronic warfare pocket guide. Norwich, CT: SciTech Publishing, 2013.
M. Barkat, "Signal detection and estimation, Artech House," Boston & London, 2005.
H. Poor, An introduction to signal detection and estimation. Springer Science & Business Media, 1998.
Q. I. Bingbing, "DOA estimation of the coherent signals using beamspace matrix reconstruction," Signal Processing, vol. 191, 2022.
L. C. Godara, "Beamforming in the presence of correlated arrivals using structured correlation matrix," IEEE Trans. Acoust., vol. 38, no. 1, pp. 1–15, 1990.
C.-C. Keh-Chiarng, "A unitary transformation method for angle-of-arrival estimation," IEEE Transactions on Signal Processing, vol. 39, pp. 975–977, 1991.
S. U. Pillai and B. H. Kwon, "Forward/backward spatial smoothing techniques for coherent signal identification," IEEE Trans. Acoust., vol. 37, no. 1, pp. 8–15, 1989.
H. B. Lee and M. S. Wengrovitz, "Resolution threshold of beamspace MUSIC for two closely spaced emitters," IEEE Trans. Acoust., vol. 38, no. 9, pp. 1545–1559, 1990.
A. Y. Hassan and S. M. Shaaban, "Enhancement of noise performance in digital receivers by over sampling the received signal," International Journal of Industrial Mathematics, vol. 6, pp. 275–284, 2014.
W. Kester, "Oversampling Interpolating DACs," Analog.com. [Online]. Available: https://www.analog.com/media/en/training-seminars/tutorials/mt-017.pdf. [Accessed: 08-Jul-2023].
C.-L. Liu and P. P. Vaidyanathan, "Super nested arrays: Linear sparse arrays with reduced mutual coupling—part I: Fundamentals," IEEE Trans. Signal Process., vol. 64, no. 15, pp. 3997–4012, 2016.

Appendix A

In this appendix CRB for AOA estimation using ULA is derived. From equation (1), conditional probability density function (PDF) can be written as follows:

$$P(\mathbf{X} \mid \theta) = \text{const} * e^{-\left(\frac{(\mathbf{X}-\mathbf{a}(\theta)\mathbf{s})^H(\mathbf{X}-\mathbf{a}(\theta)\mathbf{s})}{\sigma^2}\right)} \quad \text{A1}$$

Where (const) expresses a constant term. since J samples represent i.i.d. random variables, then

$$\begin{aligned} P(\mathbf{X} \mid \theta) &= \prod_{l=1}^{J} \text{const} * e^{-\left(\frac{(\vec{x}_l-\mathbf{a}(\theta)s_l)^H(\vec{x}_l-\mathbf{a}(\theta)s_l)}{\sigma^2}\right)} \\ &= \left(\prod_{l=1}^{J} \text{const}\right) * e^{-\frac{1}{\sigma^2}\sum_{l=1}^{J}(\vec{x}_l-\mathbf{a}(\theta)s_l)^H(\vec{x}_l-\mathbf{a}(\theta)s_l)} \\ &= (\text{const}) * e^{-\frac{1}{\sigma^2}\sum_{l=1}^{J}(\vec{x}_l-\mathbf{a}(\theta)s_l)^H(\vec{x}_l-\mathbf{a}(\theta)s_l)} \end{aligned} \quad \text{A2}$$

Equation (A2) in logarithmic form can be written as:

$$\begin{aligned} \ln P(\mathbf{X} \mid \theta) &= \ln \text{const} + \frac{-1}{\sigma^2}\left(\sum_{l=1}^{J}(\vec{x}_l - \mathbf{a}(\theta)s_l)^H(\vec{x}_l - \mathbf{a}(\theta)s_l)\right) \\ &= \text{const} + \frac{1}{\sigma^2}\sum_{l=1}^{J}[-(\vec{x}_l^H\vec{x}_l) - ((\mathbf{a}(\theta)s_l)^H\mathbf{a}(\theta)s_l) \\ &\quad + \vec{x}_l^H(\mathbf{a}(\theta)s_l) + (\mathbf{a}(\theta)s_l)^H\vec{x}_l] \end{aligned} \quad \text{A3}$$

After some simple mathematical manipulations, equation (A3) can be written as:

$$\begin{aligned} \ln P(\mathbf{X} \mid \theta) &= \text{const} + \frac{1}{\sigma^2}\sum_{l=1}^{J}[-\vec{x}_l^H\vec{x}_l \\ &\quad - s_l^*\mathbf{a}(\theta)^H\mathbf{a}(\theta)s_l + \vec{x}_l^H\mathbf{a}(\theta)s_l + s_l^*\mathbf{a}(\theta)^H\vec{x}_l] \end{aligned} \quad \text{A4}$$

Fisher information equation can be written as follows[19,20]

$$I(\theta) = -E\left[\frac{\partial^2}{\partial\theta^2}\log P(\mathbf{X} \mid \theta)\right] \quad \text{A5}$$

The first derivative of A4 w.r.t θ will be:

$$\begin{aligned} \frac{\partial}{\partial\theta}\log P(\mathbf{X} \mid \theta) &= \frac{1}{\sigma^2}\sum_{l=1}^{J}[-s_l^*\mathbf{a}'(\theta)^H\mathbf{a}(\theta)s_l \\ &\quad -s_l^*\mathbf{a}(\theta)^H\mathbf{a}'(\theta)s_l + \vec{x}_l^H\mathbf{a}'(\theta)s_l + s_l^*\mathbf{a}'(\theta)^H\vec{x}_l] \end{aligned} \quad \text{A6}$$

Then the second derivative will be

$$\frac{\partial^2}{\partial\theta^2}\log P(\mathbf{X}\mid\theta)=\frac{1}{\sigma^2}\sum_{l=1}^{J}[-s_l^*\mathbf{a}''(\theta)^H\mathbf{a}(\theta)s_l-s_l^*\mathbf{a}'(\theta)^H\mathbf{a}'(\theta)s_l-s_l^*\mathbf{a}'(\theta)^H\mathbf{a}'(\theta)s_l \\ -s_l^*\mathbf{a}(\theta)^H\mathbf{a}''(\theta)s_l+\vec{x}_l^H\mathbf{a}''(\theta)s_l+s_l^*\mathbf{a}''(\theta)^H\vec{x}_l] \quad \text{A7}$$

After taking expectation of 1 and then substituting in A7, the result will be

$$\frac{\partial^2}{\partial\theta^2}\log P(\mathbf{X}\mid\theta)=\frac{1}{\sigma^2}\sum_{l=1}^{J}[-s_l^*\mathbf{a}''(\theta)^H\mathbf{a}(\theta)s_l-s_l^*\mathbf{a}'(\theta)^H\mathbf{a}'(\theta)s_l-s_l^*\mathbf{a}'(\theta)^H\mathbf{a}'(\theta)s_l \\ -s_l^*\mathbf{a}(\theta)^H\mathbf{a}''(\theta)s_l+s_l^*\mathbf{a}(\theta)^H\mathbf{a}''(\theta)s_l+s_l^*\mathbf{a}''(\theta)^H\mathbf{a}(\theta)s_l] \quad \text{A8}$$

$$\frac{\partial^2}{\partial\theta^2}\log P(\mathbf{X}\mid\theta)=\frac{1}{\sigma^2}\sum_{l=1}^{J}-2s_l^*\mathbf{a}'(\theta)^H\mathbf{a}'(\theta)s_l \\ =\frac{-2J\mathbf{a}'(\theta)^H\mathbf{a}'(\theta)S_p}{\sigma^2} \quad \text{A9}$$

Where *Sp* is the signal power and a(θ) is the steering vector and can be redefined as follows:

$$\mathbf{a}(\theta)=\left[1,e^{-i2\pi F_c\frac{d\sin(\theta)}{C}},\dots,e^{-i2\pi F_c\frac{(M-1)d\sin(\theta)}{C}}\right]^T \quad \text{A10}$$

Where K = $2\pi/\lambda_c$ is the propagation constant. Then by calculating the derivative of the steering vector a(θ) w.r.t angle of arrival, θ, we get that:

$$\mathbf{a}'(\theta)=-jKd\cos(\theta)\left[0,\dots,(m-1)e^{-i2\pi F_c\frac{(m-1)d\sin(\theta)}{C}},\right. \\ \left.\dots\dots,(M-1)e^{-i2\pi F_c\frac{(M-1)d\sin(\theta)}{C}}\right]^T \quad \text{A11}$$

$$\mathbf{a}'(\theta)^H=jKd\cos(\theta)\left[0,\dots,(m-1)e^{i2\pi F_c\frac{(m-1)d\sin(\theta)}{C}},\right. \\ \left.\dots\dots,(M-1)e^{i2\pi F_c\frac{(M-1)d\sin(\theta)}{C}}\right]^T \quad \text{A12}$$

Therefore the term a' $(\theta)^H$ a' (θ) will be:

$$\mathbf{a}'(\theta)^H\mathbf{a}'(\theta)=(Kd\cos\theta)^2\sum_{m=1}^{M}(m-1)^2 \quad \text{A13}$$

By substituting in equation (A9) and using equation (A13), we get that:

$$\frac{\partial^2}{\partial\theta^2}\log P(\mathbf{X}\mid\theta)=\frac{-2JS_p(Kd\cos(\theta))^2\sum_{m=1}^{M}(m-1)^2}{\sigma^2} \quad \text{A14}$$

Hence

$$E\left[\frac{\partial^2}{\partial\theta^2}\log\ P(\mathbf{X}\mid\theta)\right]=\frac{-2JS_p(Kd\cos(\theta))^2\sum_{m=1}^{M}(m-1)^2}{\sigma^2} \quad \text{A15}$$

So calculation of Fisher Information will be:

$$\begin{aligned} I(\theta) &= -E\left[\frac{\partial^2}{\partial\theta^2}\log\ P(\mathbf{X}\mid\theta)\right] \\ &= \frac{2JS_p(Kd\cos(\theta))^2\sum_{m=1}^{M}(m-1)^2}{\sigma^2} \end{aligned} \quad \text{A16}$$

The SNR is defined as follows:

$$\alpha=\frac{S_p}{\sigma^2} \quad \text{A17}$$

Substituting with equation (A17) in equation (A16) will give:

$$I(\theta)=2J\alpha(Kd\cos(\theta))^2\sum_{m=1}^{M}(m-1)^2 \quad \text{A18}$$

Since the relation between CRB and fisher information can defined as in[19,20] as:

$$CRB\geq I^{-1} \quad \text{A20}$$

Appendix B

After applying the pre-processing stage and replacing σ with σ ˜, the conditional PDF $P(\mathbf{X}\mid\theta)$ will be :

$$P(\mathbf{X}\mid\theta)=\ \text{const}\ *e^{\left(\frac{(\mathbf{X}-\mathbf{a}(\theta)\mathbf{s})^H(\mathbf{X}-\mathbf{a}(\theta)\mathbf{s})}{\tilde{\sigma}^2}\right)} \quad \text{B21}$$

Where $\tilde{\sigma}^2$ is the effective noise variance after applying the pre-processing stage

$$P(\mathbf{X}\mid\theta)=(\ \text{const}\ )*e^{-\frac{1}{\tilde{\sigma}^2}\sum_{l=1}^{k}(\vec{x}_l-\mathbf{a}(\theta)s_l)^H(\vec{x}_l-\mathbf{a}(\theta)s_l)} \quad \text{B22}$$

The logarithmic form will be:

$$\begin{aligned} \ln\ P(\mathbf{X}\mid\theta) &= \text{const}+\frac{1}{\tilde{\sigma}^2}\sum_{l=1}^{J}[-\vec{x}_l^H\vec{x}_l-s_l^*\mathbf{a}(\theta)^H\mathbf{a}(\theta)s_l \\ &+\vec{x}_l^H\mathbf{a}(\theta)s_l+s_l^*\mathbf{a}(\theta)^H\vec{x}_l \end{aligned} \quad \text{B23}$$

Taking the second derivative for ln $P(\mathbf{X} \mid \theta)$ w.r.t. θ and following the same procedures as proven previous in appendix A, we get that:

$$\frac{\partial^2}{\partial\theta^2}\log P(\mathbf{X} \mid \theta) = \frac{1}{\sigma^2}\sum_{l=1}^{J}\left[-s_l^*\mathbf{a}''(\theta)^H\mathbf{a}(\theta)s_l - s_l^*\mathbf{a}'(\theta)^H\mathbf{a}'(\theta)s_l - s_l^*\mathbf{a}'(\theta)^H\mathbf{a}'(\theta)s_l - s_l^*\mathbf{a}(\theta)^H\mathbf{a}''(\theta)s_l + s_l^*\mathbf{a}(\theta)^H\mathbf{a}''(\theta)s_l + s_l^*\mathbf{a}''(\theta)^H\mathbf{a}(\theta)s_l\right] \quad \text{B24}$$

$$\frac{\partial^2}{\partial\theta^2}\log P(\mathbf{X} \mid \theta) = \frac{-2JS_p(Kd\cos(\theta))^2\sum_{m=1}^{M}(m-1)^2}{\tilde{\sigma}^2} \quad \text{B25}$$

Getting the expectation of equation (B25) we get the fisher information as follows:

$$\begin{aligned} I(\theta) &= -E\left[\frac{\partial^2}{\partial\theta^2}\log P(\mathbf{X} \mid \theta)\right] \\ &= \frac{2JS_p(Kd\cos(\theta))^2\sum_{m=1}^{M}(m-1)^2}{\tilde{\sigma}^2} \end{aligned} \quad \text{B26}$$

Substitute with equation (12) in equation (B26)

$$I(\theta) = \frac{2JRS_p(Kd\cos(\theta))^2\sum_{m=1}^{M}(m-1)^2}{\sigma^2} \quad \text{B27}$$

Substitute with equation (A17) in equation (B27), Then:

$$I(\theta) = 2JR\alpha(Kd\cos(\theta))^2\sum_{m=1}^{M}(m-1)^2 \quad \text{B28}$$

Hence, by using equation (A19), we can define the CRB after applying the proposed scheme as follows:

$$\begin{aligned} CRB &\geq \frac{1}{2J(R\alpha)(Kd\cos(\theta))^2\sum_{m=1}^{M}(m-1)^2} \\ &= \frac{1}{2J\tilde{\alpha}(Kd\cos(\theta))^2\sum_{m=1}^{M}(m-1)^2} \end{aligned}$$

Equation (B29) confirms that CRB is reduced by amount equal to OSR.

Appendix C

C.1. Detection Range

Figure 2 indicates two targets SOI_1 and SOI_2 which are close to each other. The aim is to correctly resolve the two targets and estimate their AOAs correctly although the far distance between them and DF receiver due to the physical barrier existed between them.

As indicated in[18], the effective distance between receiver and targets, in the case of LOS propagation, is described as follows:

$$20\log\ d_1 = P_T + G_T + G_R - 32.44 - 20\log\ F_c - S_p \quad \text{C30}$$

and

$$\alpha = S_p - \sigma^2 \quad \text{C31}$$

Substitute with equation (C31) in equation (C30)

$$20\log\ d_1 = P_T + G_T + G_R - 32.44 - 20\log\ F_c - \alpha - \sigma^2 \quad \text{C32}$$

After applying "Over-Sampling and Averaging", the effective noise variance will be reduced by the pre-processing gain as follows:

$$\tilde{\sigma}^2 = \frac{\sigma^2}{R} \quad \text{C33}$$

Hence in logarithmic form it will be:

$$\tilde{\sigma}^2 = \sigma^2 - 10\log\,(R) \quad \text{C34}$$

After applying equation (C34) in equation (C32), the maximum distance after will defined as follows:

$$\begin{aligned} 20\log\ d_2 &= P_T + G_T + G_R - 32.44 - 20\log\ F_c - \alpha_{dB} - \tilde{\sigma}^2 \\ &= P_T + G_T + G_R - 32.44 - 20\log\ F_c - \alpha_{dB} - \sigma^2 + 10\log\,(R) \end{aligned} \quad \text{C35}$$

$$20\log\ d_2 = (20\log\ d_1) + 10\log\,(R) \quad \text{C36}$$

Equation (C36) confirms that after applying the pre-processing stage the maximum effective distance will increase with a factor equal to the pre-processing gain [10log (R)]

C.2. Processing gain

Noise variance reduction due to the pre-processing stage will increase the SNR by a factor equals the processing gain. Signal-to-noise-ratio (in dB) before applying the proposed scheme can defined as follows:

$$\alpha = S_p - \sigma^2 \quad \text{C37}$$

Where S_p and σ^2 are signal power and noise variance, noise power, respectively. After applying the pre-processing stage the effective noise variance will be reduced as in equation(C34) and the effective SNR will be:

$$\begin{aligned} \tilde{\alpha} &= S_p - \tilde{\sigma}^2 \\ &= S_p - \sigma^2 + 10\log\ R \\ &= \alpha + 10\log\ R \end{aligned} \quad \text{C38}$$